Carbohydrate Polymers 103 (2014) 32–37

Contents lists available at ScienceDirect

Carbohydrate Polymers

journal homepage: www.elsevier.com/locate/carbpol

Tailored functionalization of ZnO nanoparticle via reactive cyclodextrin and its bionanocomposite synthesis

Amir Abdolmaleki[a,b,*], Shadpour Mallakpour[a,b,*], Sedigheh Borandeh[a]

[a] Organic Polymer Chemistry Research Laboratory, Department of Chemistry, Isfahan University of Technology, Isfahan 84156-83111, Islamic Republic of Iran
[b] Nanotechnology and Advanced Materials Institute, Isfahan University of Technology, Isfahan 84156-83111, Islamic Republic of Iran

ARTICLE INFO

Article history:
Received 7 August 2013
Received in revised form 3 November 2013
Accepted 4 December 2013
Available online 12 December 2013

Keywords:
Monochlorotriazinyl-β-cyclodextrin (MCT-β-CD)
Surface modification
Bionanocomposite
Amino acid

ABSTRACT

β-cyclodextrin was grafted onto the surface of ZnO nanoparticles via efficient, simple and fast technique through nucleophilic substitution reaction of OH groups on ZnO nanoparticle surface with reactive cyclic oligosaccharide, Monochlorotriazinyl-β-cyclodextrin (MCT-β-CD). Characterization of functionalized ZnO nanoparticles were carried out by Fourier transform infrared spectra (FT-IR), elemental analysis (CHN), Thermogravimetric analysis (TGA), X-ray diffraction (XRD), field emission scanning electron microscopy (FE–SEM) and transmission electron microscopy (TEM). The amount of MCT-β-CD bonded to the ZnO surface was determined by CHN and TGA analysis. Followed by, innovative poly(ester-amide)/ZnO bionanocomposites (PEA/ZnO BNCs) were fabricated through solution mixing method. Due to using biodegradable amino acid containing polymer, the synthesized nanocomposites are expected to classify as biologically active materials. Morphological studies of prepared BNC proved good distribution of modified ZnO in PEA matrix with nanoscale size. Good dispersion and less aggregation, indicate the effect of functionalization on preventing nanoparticles to aggregate.

1. Introduction

Throughout recent years, it has been demonstrated that inorganic moieties play an important role in improvement of the membrane performance composed of polymer matrix and inorganic nanoparticles (Koo, 2006; Lau, Hussain, & Lafdi, 2009). Nanoscale structure effects of inorganic materials and strong interfacial interaction between polymer matrix and them, significantly lead to improve their properties. Nevertheless, due to the incompatibility of inorganic nanoparticles with organic matrix and their tendency to aggregate, the many valuable properties of nanoparticles will not be available entirely. Therefore, some modifications were needed to turn the surface of nanoparticles from hydrophilic to organophilic (Abdolmaleki, Mallakpour, & Borandeh, 2012a; Mallakpour & Madani, 2012; Tang, Liu, Sun, Zheng, & Cheng, 2007). Furthermore, among several modifier molecules, environmentally friendly types are preferred to overcome global pollution.

Cyclodextrins (CDs) are a category of cyclic toroidal-shaped oligosaccharides with a hydrophilic exterior surface and a hydrophobic hollow interior (Villalonga, Cao, & Fragoso, 2007). They are environmentally friendly and commonly used in textile, packaging, cosmetics and food industries (Del Valle, 2004; Hedges, 1998; Shahid ul, Shahid, & Mohammad, 2013). In addition, CDs represent a great potential to be used in novel applications, particularly in biologically active guest area, such as drug delivery and antimicrobial agents and insect repellents (Arima, Motoyama, & Higashi, 2012; Jin, Liu, Sun, Ni, & Wei, 2010; Rasheed & Kumar, 2008). Quite a number of nanostructural compounds and composites have been fabricated through CDs' self-assembly, and its hydroxyl groups are also known to make compatibility with inorganic-oxide or polymer matrixes through different variety of interactions. So CDs are appropriate candidates which can be used as a biosafe and environmentally friendly modifiers (Badruddoza, Hidajat, & Uddin, 2010; Badruddoza, Shawon, Tay, Hidajat, & Uddin, 2013; Kiasat & Nazari, 2012; Kim & Nichols, 2012; Shown, Ujihara, & Imae, 2010).

Among CD's derivatives, monochlorotriazinyl-β-cyclodextrin (MCT-β-CD) having a monochlorotriazinyl group as a reactive anchor, was introduced to have capability of forming covalent bonds with nucleophilic substituents, such as –OH or $–NH_2$ groups (Abdel-Halim, Abdel-Mohdy, Al-Deyab, & El-Newehy, 2010; Ibrahim, E-Zairy, & Eid, 2010; Ibrahim & El-Zairy, 2009; Rehmann, Yoshii, & Furuta, 2003). Therefore, MCT-β-CD provides an interesting way of surface modification for inorganic nanomaterials.

Accordingly, the present work is directed towards an efficient method of ZnO nanoparticle surface modification using

* Corresponding authors. Tel.: +98 311 391 3249/+98 311 391 3267; fax: +98 3113912350.
E-mail addresses: abdolmaleki@cc.iut.ac.ir, amirabdolmaleki@yahoo.com, abdolmalek@gmail.com (A. Abdolmaleki), mallak@cc.iut.ac.ir, mallak777@yahoo.com, mallakpour84@alumni.ufl.edu (S. Mallakpour).

0144-8617/$ – see front matter © 2013 Elsevier Ltd. All rights reserved.
http://dx.doi.org/10.1016/j.carbpol.2013.12.013

MCT-β-CD for attaining high-performance dispersible nanoparticles. This reactive CD derivative was selected due to its commercial accessibility, antibacterial property and having no irritating or sensitizing effects. The introduction of β-CD onto ZnO surface could inhibit the aggregation of ZnO nanoparticles. Afterwards, polymer/ZnO bionanocomposites (BNCs) were fabricated by biodegradable amino acid containing poly(ester-amide) (PEA) and synthesized functionalized ZnO (f-ZnO). Prepared materials were characterized with several techniques. Microscopic characterization (FE–SEM and TEM), proved well dispersion of f-ZnO in the polymer matrix with nanoscale size. This newly developed strategy provides a good example of covalently β-CD functionalized nanoparticle application in high-performance nanocomposite synthesis.

2. Experimental

2.1. Materials

MCT-β-CD was purchased from Ebo-chem. Nano-ZnO particle with an average particle size of about 25–30 nm was purchased from Neutrino Co. *N*,*N*′-dimethylformamide (DMF), Na_2CO_3 and NaCl were purchased from Merck Co. DMF as solvent was distilled over barium oxide under reduced pressure. Other reagents were used without further purification.

2.2. Functionalization of ZnO nanoparticles with MCT-β-CD

0.1 g dry ZnO nanoparticles, 0.025 g MCT-β-CD, 4 mL H_2O and 0.015 g Na_2CO_3 were heated to 98 °C for 90 min. At 30 and 60 min 0.015 g NaCl and at 90 min 0.015 g Na_2CO_3 were added. The reaction temperature was hold for 2 h. The product was filtered and washed several times with water, eventually dried under vacuum at 70 °C for 24 h. The reaction schematic was shown in Scheme 1.

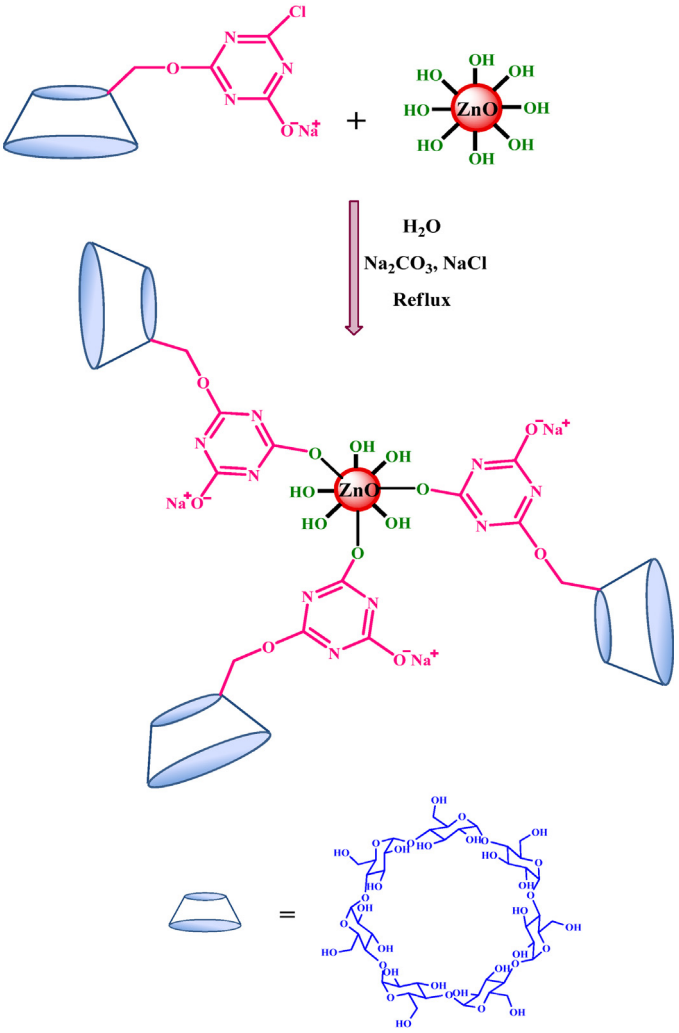

Scheme 1. Modification of ZnO nanoparticles with MCT-β-CD.

2.3. Polymer synthesis

Synthesis of poly(ester-amide) (PEA) which is briefly described, was carried out through our previous work (Abdolmaleki, Mallakpour, Borandeh, & Sabzalian, 2012b): 0.5 mmol (0.26 g) *N*,*N*′-bis[2-(methyl 3-(4-hydroxyphenyl)propanoate)] isophthaldiamide (diol) and 3 mmol (0.4 mL) TEA were dissolved in NMP (2 mL) at room temperature. To this solution, 0.5 mmol (0.1 g) isophthaloyl dichloride was added in one portion. Then it was stirred at room temperature for 12 h and was poured into 50 mL of methanol. The precipitate was filtered off and washed with methanol. Powdered polymer was dried at 80 °C for 12 h under vacuum. The structure of polymer is shown in Scheme 2.

2.4. Synthesis of PEA/f-ZnO BNCs

To achieve uniformly mixed PEA/f-ZnO solutions with desired weight percentages of f-ZnO, a two-step method was used. First,

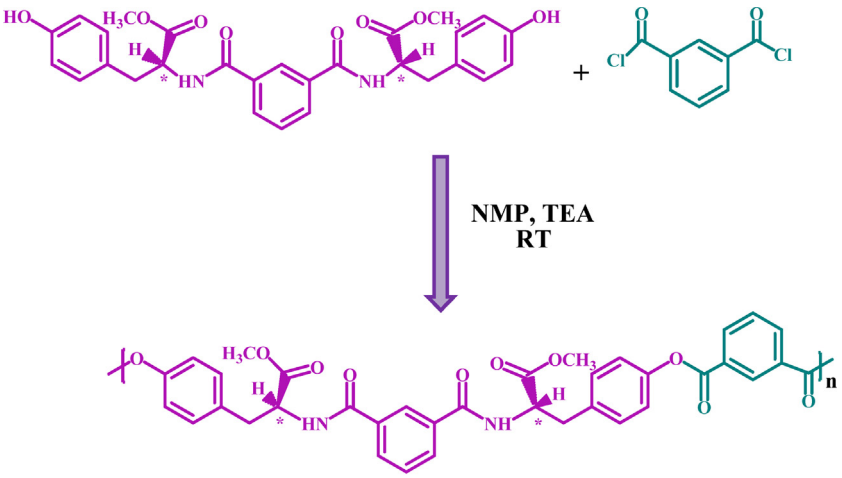

Scheme 2. Synthesis of PEA.

two stock solutions were prepared: 0.1 g PEA was dissolved in 2 mL DMF and f-ZnO was separately dispersed in 2 mL DMF solution and stirring for 1 day at ambient temperature. Then; two stock solutions were mixed to achieve the desired weight percentages of f-ZnO (4, 8 and 12 wt%). The PEA/f-ZnO solutions were stirred for 1 day at room temperature and then ultrasonicated in water bath for 1 h. To remove the DMF solvent, PEA/f-ZnO solutions were poured into an uncovered preheated glass Petri for 1 day; then the semidried solids were further dried in vacuum at 160 °C for 8 h.

2.5. Measurements

FT-IR spectra of the composites were recorded on Jasco-680 (Japan) spectrometer at 4 cm^{-1} resolution by using pressed KBr pellets, and scanned at wavenumber range 400–4000 cm^{-1}. Elemental analyses were performed by a CHNS-932, Leco. Thermogravimetric analysis (TGA) is performed with a STA503 win TA (Bahr-Thermoanalyse GmbH, Hüllhorst, Germany) at the heating rate of 10 °C/min from 25 to 800 °C under nitrogen atmosphere. X-ray diffraction (XRD) was used to characterize the crystalline structure of composites. XRD patterns were collected using a Bruker, D8 Advanced diffractometer with a copper target at the wave length λ Cu$K\alpha$ = 1.54 Å and a tube voltage of 40 kV and tube current of 35 mA, in the range of 10–100° at the speed of 0.05°/min. Nanocomposite morphology was observed using field emission scanning electron microscopy (FE-SEM, HITACHI S-4160, Japan). Transmission electron microscopy (TEM) image was obtained using Philips CM 120 operated (Netherlands) at voltage of 150 kV.

3. Results and discussions

3.1. Functionalization of ZnO nanoparticles

For improving the mechanical and thermal properties of polymer, ZnO nanoparticles were inserted into polymer matrix, but physical forces like van der Waals interactions lead to nanoparticle agglomeration. Consequently, to avoid this occurrence and attain homogeneous distribution of ZnO nanoparticles in the polymer matrix, ZnO surface must be characteristically organophile to have close affinity to organic matrix. Monochlorotriazinyl-β-cyclodextrin (MCT-β-CD), a biologically active compound, having a monochlorotriazinyl group as a reactive anchor, is able to form covalent bonds to nucleophilic substituents, like –OH groups. So ZnO nanoparticles were modified with MCT-β-CD as a coupling agent to functionalize the surface of them. Each O–H group of ZnO surface can react with reactive triazine Cl leaving group. Therefore, MCT-β-CD molecules are grafted onto ZnO nanoparticle surface. Furthermore, the organic chains of MCT-β-CD can make steric hindrance between inorganic nanoparticles to reduce their agglomeration. The proposed interactions of ZnO nanoparticles modified with MCT-β-CD are illustrated in Scheme 1.

3.2. Characterization of f-ZnO nanoparticles

3.2.1. FT-IR study

To confirm the covalent functionalization of ZnO nanoparticle with MCT-β-CD, its structure was examined by FT-IR analysis. Fig. 1(A) shows FT-IR spectra of pure ZnO, MCT-β-CD and f-ZnO. In pure ZnO spectrum (a), –OH groups at ZnO surface appear at 3434 cm^{-1} and bands at 1577 and 1384 cm^{-1} correspond to asymmetric and symmetric C=O stretching modes of zinc acetate. In addition the peak at the region of 430 cm^{-1} is attributed to the Zn–O stretching of ZnO. In MCT-β-CD spectrum (b), significant peaks attributed to –OH groups (3420 cm^{-1}), C=N and C–N triazine ring (1611 and 1469 cm^{-1}). In comparison to f-ZnO spectrum of

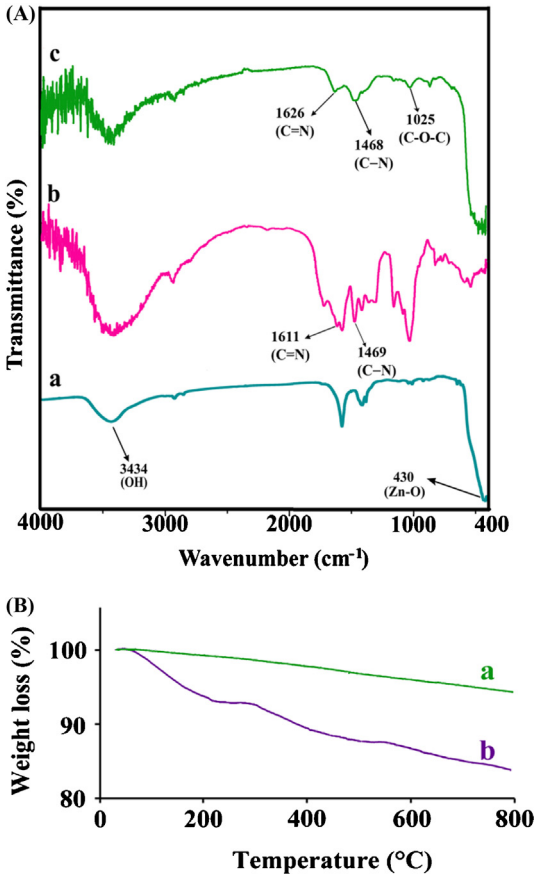

Fig. 1. (A) FT-IR spectra of pure ZnO (a), MCT-β-CD (b) and f-ZnO (c) and (B) TGA curves of pure ZnO (a) and f-ZnO (b).

(c) and pure ZnO (a), the existence of characteristic peaks including C=N and C–N triazine ring (1626 and 1468 cm^{-1}) and C–O–C (1025 cm^{-1}), verify grafting of MCT-β-CD onto surface of ZnO nanoparticles.

3.2.2. TGA analysis

TGA has been used as a useful tool to determine the quantitative contents of grafted MCT-β-CD onto ZnO surface. The TGA curves of pure ZnO and f-ZnO are shown in Fig. 1(B). According to the TGA curve of f-ZnO (b), an important weight loss starting at 300 °C was observed which is attributed to the decomposition of MCT-β-CD moieties. Furthermore, the weight variation for $T < 200$ ascribed to the loss of physisorbed water by CD molecules due to their hydroxyl groups present on their external face (Nielsen, Kingshott, Uyar, Hacaloglu, & Larsen, 2011; Ponchel et al., 2004). The weight loss differences between pure ZnO (a) and f-ZnO (b) can be attributed to pyrolyzed MCT-β-CD. Based on TGA results, the MCT-β-CD content of f-ZnO is found to be 77.8 μmol/g ZnO.

3.2.3. CHN analysis

To verify the functionalization of ZnO nanoparticles by MCT-β-CD and estimate the amount of MCT-β-CD bonded to ZnO surface, CHN analysis was used. CHN analysis provides elemental concentration of carbon, hydrogen and nitrogen before and after functionalization of ZnO nanoparticle (Table 1). These data confirm MCT-β-CD grafting onto ZnO nanoparticle surface. By means of f-ZnO nitrogen content measuring, the amount of MCT-β-CD grafted

Table 1
CHN data before and after functionalization of ZnO nanoparticles.

Sample	C%	N%	H%
Pure ZnO	0.554	0.000	0.487
f-ZnO	1.310	0.251	0.392

onto the ZnO surface was calculated through the following equation (Nielsen et al., 2011):

$$\frac{\text{mol}}{g} = \frac{\left(W_t \times 100/X\right) \times 100/100 - \left(W_t \times 100/X\right)}{Y}$$

where W_t is the weight percent of the element measured, X is the theoretical weight percent of the element in the molecule and Y is the theoretical M_w of the molecule. MCT-β-CD has carbon, hydrogen and nitrogen contents of 42.01, 5.41 and 3.27 wt% with a M_w of 1285.32 g/mol. Based on this equation, the amount of MCT-β-CD detected from nitrogen contents is 64.6 μmol/g.

3.2.4. Stability of the hybrids in distilled water

As a result of MCT-β-CD grafting onto ZnO nanoparticles, the dispersibility of f-ZnO was dramatically high. For a better understanding, a digital photograph of ZnO nanoparticle dissolved in distilled water before and after functionalization is shown in Fig. 2(A). Pure ZnO (left) does not have dispersion stability in water and precipitate at the bottom of the vial because of their tendency to aggregates. In the case of functionalization by MCT-β-CD, the dispersion ability is much improved and excellent stability in water is observed which f-ZnO is homogeneously dispersed (right). From homogeneous solution, it is obvious that there must be MCT-β-CD residing on ZnO nanoparticle surface, which improve their organophilicity.

3.2.5. Surface morphology analysis (FE–SEM and TEM)

For more consideration, the surface morphology and particle dimensions of synthesized f-ZnO were examined by FE–SEM and TEM analysis. FE–SEM micrographs of f-ZnO nanoparticles

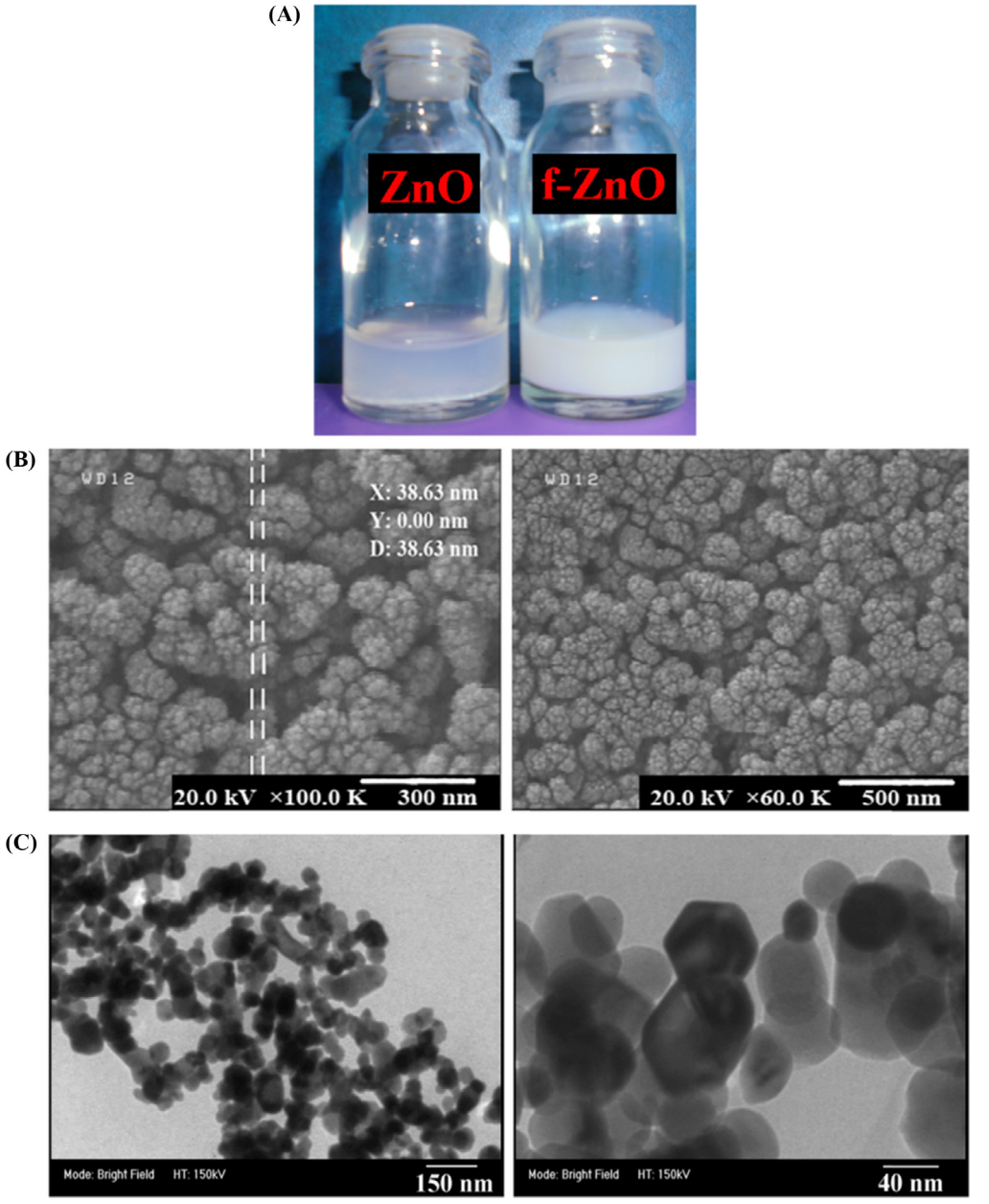

Fig. 2. (A) Photograph of aqueous dispersion of pure ZnO (left) and f-ZnO (right), (B) FE–SEM and (C) TEM micrographs of f-ZnO.

(Fig. 2(B)) proved that they are in nanoscale range and have a uniform distribution with spherical shape. Moreover, less aggregation was observed, indicating the effectiveness of functionalization for prevention of aggregation.

Additionally, the TEM images (Fig. 2(C)) also confirm good distribution of f-ZnO in nanoscale range (10–40 nm). It is obvious that, the surface property of ZnO nanoparticles is evidently became organophilic by using MCT-β-CD as modifier and also the organic chains of MCT-β-CD can make steric hindrance between inorganic nanoparticles and reduce agglomeration of ZnO nanoparticles that lead to excellent distribution.

3.3. PEA/f-ZnO BNCs preparation

After ZnO nanoparticle functionalization by biosafe β-CD derivative (MCT-β-CD), its polymer BNCs was fabricated via solution mixing method. To this aim, a biodegradable amino acid containing PEA was used as a polymer matrix. For preparing PEA/ZnO BNCs, the dispersion of f-ZnO (4, 8, and 12 wt%) in PEA was achieved by a vigorous stirring for 1 day (in DMF), followed by an ultrasonication process for 1 h to form a new series of chiral BNCs. The valuable employing amount of ZnO nanoparticles in composite depends on the ability to uniform disperse throughout the polymer matrix without reducing their aspect ratio. But ZnO, due to its hydrophilic surface and having high specific surface area and surface energy, cannot disperse uniformly in polymer matrix, which causes some phase separation and aggregation in ZnO nanoparticles. Therefore, they have very low solubility in solvents and tend to remain as entangled agglomerates. To overcome the difficulty of dispersion, ZnO surface was organophiled by MCT-β-CD which containing several different functional groups in its chain and can make possible interactions between PEA chains and lead to a good dispersion and compatibility with polymer matrix.

3.4. Characterization of BNCs

3.4.1. FT-IR study

FT-IR spectra were used to study chemical structure of the pure PEA and PEA/ZnO BNCs (4, 8 and 12 wt%) (Fig. 3). Characteristic peaks in PEA spectrum are 3408 (N–H), 1741 (C=O ester), 1663 (C=O amide), 1299 (C–N), 1221 (C–O). As it was explained in FT-IR spectrum of f-ZnO, outstanding peaks are attributed to C=N and Zn–O–Zn groups. As it can be seen, all these significant peaks appeared in the BNCs spectra and also the Zn–O–Zn absorbance intensity increased by increasing of f-ZnO content. Furthermore, the peak at 1663 cm^{-1} became broad with enhancing of f-ZnO content due to overlaying of C=N groups in f-ZnO and amidic C=O groups in PEA. These results revealed the success in synthesizing PEA/ZnO BNCs.

3.4.2. XRD analysis

Fig. 4 shows X-ray patterns of pure PEA, f-ZnO nanoparticles and BNCs (4, 8 and 12 wt%) in the region of $2\theta = 10–100^{\circ}$. The broad peak in XRD curve of PEA shows the amorphous nature of PEA in absence of ZnO nanoparticles, meaning that there are no regular crystalline planes to XRD. XRD patterns of f-ZnO nanoparticles have been indexed to the hexagonally wurtzite structured ZnO, which is in accord with the standard values for ZnO given in International Center for diffraction data, JCPDS (no. 36-1451). XRD patterns of PEA/ZnO BNCs demonstrated peaks of ZnO and PEA and also proved that the morphology of ZnO nanoparticles has not been changed during the process. The obtained data from XRD analysis exhibited that all prepared BNCs have similar XRD patterns, but there is only a little difference appeared in XRD patterns, which could be associated with the content of ZnO nanoparticles in BNC structures. With comparing of BNCs' spectra it was observed that with enhancement

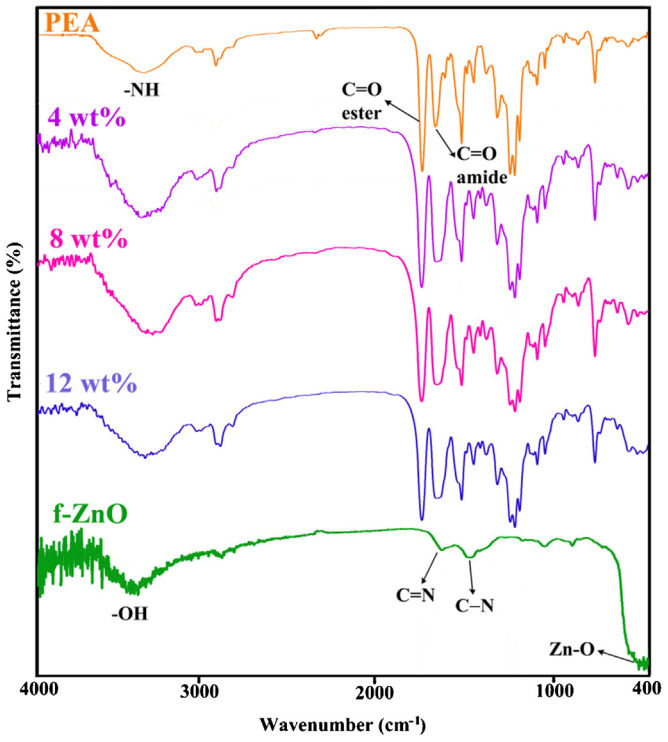

Fig. 3. FT-IR spectra of PEA, f-ZnO and PEA/ZnO BNCs (4, 8 and 12 wt%).

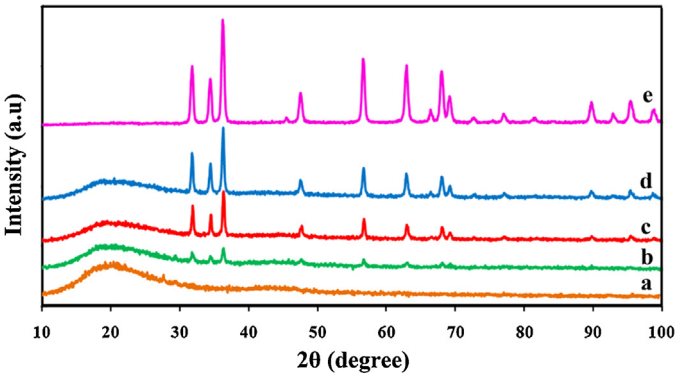

Fig. 4. XRD patterns of PEA (a), PEA/ZnO BNCs ((b) 4 wt%, (c) 8 wt% and (d) 12 wt%) and f-ZnO (e).

of ZnO contents in BNCs, the intensity of crystalline peaks was gradually increased. The XRD results also confirm that introduction of β-CD can prevent aggregation of nanoparticles. The average size of the ZnO nanoparticles in BNCs is calculated to be 25–30 nm consistent with the Debye–Scherrer formula ($D = 0.9\,\lambda/\beta\cos\theta$).

3.4.3. Microscopy characterization

To characterize the morphology and dispersity of f-ZnO in polymer matrix; FE–SEM images of fracture surfaces of pure PEA and PEA/ZnO BNC (12 wt%) were examined as demonstrated in Fig. 5. As seen, PEA consists of both micro and nano spherical-shaped structures and its morphology is amorphous (Fig. 5(a) and (b)). Fig. 5(c) and (d) show the FE–SEM micrographs of PEA/ZnO BNC (12 wt%). From these photographs, it was observed that f-ZnO nanoparticles were well dispersed in the polymer matrix, because, f-ZnO nanofiller having outstanding adhesion and strong interfacial bonding to PEA. As it is observed, f-ZnO nanoparticles are homogeneously dispersed in the polymer matrix and their sizes are estimated to be between 20 and 50 nm.

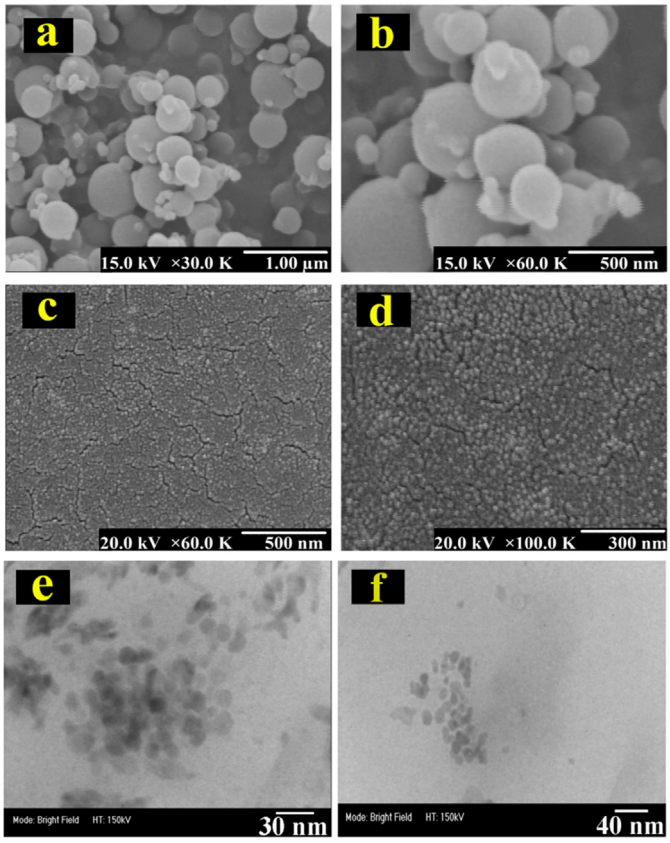

Fig. 5. FE-SEM images of pure PEA (a and b), PEA/ZnO BNC (12 wt%) and TEM micrographs of PEA/ZnO BNC (12 wt%).

To view the hybrid structure for prepared BNC directly, TEM analysis is used with the emphasis on dispersion of f-ZnO nanoparticles in the polymer matrix. It is a complement to XRD and SEM results. Fig. 5(e) and (f) show TEM images of PEA/ZnO BNC (12 wt%) with different scale. As it can be seen, f-ZnO nanoparticles were well dispersed in PEA matrix in nano size ranging from 10 to 30 nm. These results reveal that functionalization of ZnO nanoparticles plays an important role in formation of various interactions between functional groups in PEA chains and f-ZnO that lead to good dispersion of nanoparticles in the polymer matrix.

4. Conclusions

The results reported in this study demonstrated an efficient method to prepare β-CD covalently grafted ZnO, through a simple and direct (one-step) procedure. MCT-β-CD contains monochlorotriazinyl groups that can react with OH groups on ZnO nanoparticle surface through nucleophilic reaction. The incorporation of β-CD functional group on ZnO can prevent the aggregation of ZnO nanoparticles and also improve its compatibility with polymer matrix. The amount of MCT-β-CD grafted onto the surface of ZnO was determined by CHN and TGA analysis. The structure, morphology and size dimension of prepared f-ZnO were examined by FT-IR, XRD, FE–SEM and TEM analysis. In the next step, f-ZnO nanoparticles were employed for construction of new series of PEA/ZnO BNCs. Due to existence of numerous functional groups on the surface of f-ZnO nanoparticles; there can be possible interactions between them and PEA chains, which lead to good dispersion and compatibility with polymer matrix. Moreover, organic chains of MCT-β-CD can make steric hindrance between inorganic nanoparticles to reduce the agglomeration, which was confirmed by FE–SEM and TEM results. Based on these results ZnO nanoparticles have a good dispersion in the polymer matrix with nano size dimensions.

Acknowledgements

We gratefully acknowledge the partial financial support from the Research Affairs Division Isfahan University of Technology (IUT), Isfahan. Further partial financial support of Iran Nanotechnology Initiative Council (INIC), National Elite Foundation (NEF) and Center of Excellency in Sensors and Green Chemistry (IUT) is also gratefully acknowledged.

References

Abdel-Halim, E. S., Abdel-Mohdy, F. A., Al-Deyab, S. S., & El-Newehy, M. H. (2010). Chitosan and monochlorotriazinyl-β-cyclodextrin finishes improve antistatic properties of cotton/polyester blend and polyester fabrics. *Carbohydrate Polymers*, *82*(1), 202–208.

Abdolmaleki, A., Mallakpour, S., & Borandeh, S. (2012). The use of novel biodegradable, optically active and nanostructured poly(amide-ester-imide) as a polymer matrix for preparation of modified ZnO based bionanocomposites. *Materials Research Bulletin*, *47*(5), 1123–1129.

Abdolmaleki, A., Mallakpour, S., Borandeh, S., & Sabzalian, M. (2012). Fabrication of biodegradable poly(ester-amide)s based on tyrosine natural amino acid. *Amino Acids*, *42*(5), 1997–2007.

Arima, H., Motoyama, K., & Higashi, T. (2012). Potential use of polyamidoamine dendrimer conjugates with cyclodextrins as novel carriers for siRNA. *Pharmaceuticals*, *5*, 61–78.

Badruddoza, A. Z. M., Hidajat, K., & Uddin, M. S. (2010). Synthesis and characterization of β-cyclodextrin-conjugated magnetic nanoparticles and their uses as solid-phase artificial chaperones in refolding of carbonic anhydrase bovine. *Journal of Colloid and Interface Science*, *346*(2), 337–346.

Badruddoza, A. Z. M., Shawon, Z. B. Z., Tay, W. J. D., Hidajat, K., & Uddin, M. S. (2013). Fe_3O_4/cyclodextrin polymer nanocomposites for selective heavy metals removal from industrial wastewater. *Carbohydrate Polymers*, *91*(1), 322–332.

Del Valle, E. M. M. (2004). Cyclodextrins and their uses: A review. *Process Biochemistry*, *39*(9), 1033–1046.

Hedges, A. R. (1998). Industrial applications of cyclodextrins. *Chemical Reviews*, *98*(5), 2035–2044.

Ibrahim, N. A., E-Zairy, W. R., & Eid, B. M. (2010). Novel approach for improving disperse dyeing and UV-protective function of cotton-containing fabrics using MCT-β-CD. *Carbohydrate Polymers*, *79*(4), 839–846.

Ibrahim, N. A., & El-Zairy, E. M. R. (2009). Union disperse printing and UV-protecting of wool/polyester blend using a reactive β-cyclodextrin. *Carbohydrate Polymers*, *76*(2), 244–249.

Jin, L., Liu, Q., Sun, Z., Ni, X., & Wei, M. (2010). Preparation of 5-fluorouracil/β-cyclodextrin complex intercalated in layered double hydroxide and the controlled drug release properties. *Industrial and Engineering Chemistry Research*, *49*, 11176–11181.

Kiasat, A. R., & Nazari, S. (2012). Magnetic nanoparticles grafted with β-cyclodextrin-polyurethane polymer as a novel nanomagnetic polymer brush catalyst for nucleophilic substitution reactions of benzyl halides in water. *Journal of Molecular Catalysis A: Chemical*, *365*(0), 80–86.

Kim, J.-W., & Nichols, W. T. (2012). Hierarchically assembled titania-cyclodextrin nano-networks. *Materials Letters*, *67*(1), 11–13.

Koo, J. H. (2006). *Polymer Nanocomposites*. New York City, NY: McGraw-Hill.

Lau, A. K.-t., Hussain, F., & Lafdi, K. (2009). *Nano- and Biocomposites*. Boca Raton, London, New York: CRC Press, Taylor & Francis Group.

Mallakpour, S., & Madani, M. (2012). A facile route for the preparation of novel optically active poly(amide-imide)/functionalized zinc oxide nanocomposites containing pyromellitoyl-bis-l-phenylalanine moieties. *Polymer Bulletin*, *68*(5), 1201–1214.

Nielsen, R., Kingshott, P., Uyar, T., Hacaloglu, J., & Larsen, K. L. (2011). Characterization of β-cyclodextrin modified SiO_2. *Surface and Interface Analysis*, *43*(5), 884–892.

Ponchel, A., Abromson, S., Quartararo, J., Bormann, D., Barbaux, Y., & Monflier, E. (2004). Cyclodextrin silica-based materials: Advanced characterizations and study of their complexing behavior by diffuse reflectance UV–Vis spectroscopy. *Microporous and Mesoporous Materials*, *75*(3), 261–272.

Rasheed, A., & Kumar, A. (2008). Cyclodextrins as drug carrier molecule: A review. *Scientia Farmaceutica*, *76*, 567–598.

Rehmann, L., Yoshii, H., & Furuta, T. (2003). Characteristics of modified β-cyclodextrin bound to cellulose powder. *Starch—Stärke*, *55*(7), 313–318.

Shahid ul, I., Shahid, M., & Mohammad, F. (2013). Green chemistry approaches to develop antimicrobial textiles based on sustainable biopolymers—A review. *Industrial & Engineering Chemistry Research*, *52*(15), 5245–5260.

Shown, I., Ujihara, M., & Imae, T. (2010). Sensitizing of pyrene fluorescence by β-cyclodextrin-modified TiO_2 nanoparticles. *Journal of Colloid and Interface Science*, *352*(2), 232–237.

Tang, E., Liu, H., Sun, L., Zheng, E., & Cheng, G. (2007). Fabrication of zinc oxide/poly(styrene) grafted nanocomposite latex and its dispersion. *European Polymer Journal*, *43*(10), 4210–4218.

Villalonga, R., Cao, R., & Fragoso, A. (2007). Supramolecular chemistry of cyclodextrins in enzyme technology. *Chemical Reviews*, *107*, 3088–3116.